Geometrical Control of the Inertial Recirculation

PAOLA CESSI*

Scripps Institution of Oceanography, La Jolla, California

LUANNE THOMPSON

MIT/WHOI Joint Program in Oceanography, Woods Hole, Massachusetts

(Manuscript received 9 February 1990, in final form 4 June 1990)

ABSTRACT

In this paper we discuss the conditions under which a free solution of the steady, one-layer, quasi-geostrophic equation on a β-plane is realized in the inviscid limit. We restrict attention to the case where no body force is applied and the fluid moves under a stress prescribed at the boundary of the closed domain. We show that, depending on the geometrical configuration of the boundary where the stress is prescribed, either a frictional solution or a free inertial solution is found in the limit of infinitesimal dissipation.

1. Introduction

Despite its simplicity the steady, one-layer, wind-driven quasigeostrophic equation on a β-plane in the presence of lateral friction exhibits a rather rich behavior and can, in general, only be solved numerically. To gain insight through analytic exploration, a classical simplification is to neglect the advection of relative vorticity. If no velocity or stress is prescribed at the (closed) boundary then the amplitude of this linear solution is proportional to the forcing provided by the wind stress curl. Alternatively, the opposite limit of nonlinear, "weakly forced and dissipative" flow has been studied. Thus, the right hand side of the vorticity equation

$$J(\psi, \zeta + \beta y) = \frac{f_0 W_E}{H} + \kappa \nabla^2 \zeta \qquad (1.1)$$

where $\zeta = \nabla^2 \psi$ is, to a first approximation, neglected in comparison with the left hand side. In the oceanographic literature the classical reference is Fofonoff (1954). The solutions that satisfy the vorticity equation in the absence of forcing and dissipation are commonly termed "free" flows and have the property that $\zeta + \beta y = \mathcal{F}(\psi)$. The function $\mathcal{F}$ is determined by requiring that the circulation integrals be satisfied. Integrating (1.1) over the area $A(\psi)$ enclosed by any streamline (in a closed container all the streamlines must be closed) the advection term on the lhs vanishes exactly and

$$\int_{A(\psi)} da \, \frac{f_0 W_E}{H} = -\kappa \oint_{C(\psi)} \nabla \zeta \cdot \mathbf{dl} \qquad (1.2)$$

where $C(\psi)$ is the streamline bounding the area $A(\psi)$. In the instance where no velocity or stress is applied at the boundary the amplitude of the free solution is proportional to the forcing and inversely proportional to the frictional coefficient κ. Fofonoff (1954) examined the case where the function $\mathcal{F}(\psi)$ is linear and, assuming bottom drag as the dissipative mechanism, Niiler (1966) constructed an appropriate wind forcing that satisfies the integral constraint (1.2) and give rise to the linear function suggested by Fofonoff. In general, for a prescribed forcing it is very difficult to find the function $\mathcal{F}$ from (1.2) (see Mestel 1989, for an iterative numerical procedure), and even more difficult to determine whether such a free solution is realized in the first place. Indeed Griffa and Salmon (1989) show that the realization of free, Fofonoff-like solutions in the weakly forced and dissipative limit (in the presence of bottom drag), crucially depends on the *geometry* of the forcing. In particular, when the wind-stress curl is downward in the subtropical gyre and upward in the subpolar gyre a free solution cannot be realized, while a simple reversal in the sign of the forcing leads to a solution with two counterrotating Fofonoff-like gyres filling the whole basin. Nevertheless, in the cases where a free solution is not possible over the whole basin, a Fofonoff-like solution can be achieved in a subbasin scale region. In wind-driven numerical models such as Griffa and Salmon's (1989) we can identify a region in which potential vorticity is approximately conserved,

* Permanent affiliation: Istituto FISBAT-CNR, Bologna (Italy).

Corresponding author address: Dr. Paola Cessi, Scripps Institution of Oceanography, University of California at San Diego, Mail Code A-030, La Jolla, CA 92093.

located near the zero wind-stress curl line, where the western boundary current leaves the coast. The flow in this region is termed "inertial recirculation" and is characterized by a very large transport.

The assumption that the inertial recirculation is well described by free solutions of the quasi-geostrophic equation has been extensively used in the literature (Marshall and Nurser 1986, 1988; Greatbatch 1987; Cessi et al. 1987). Cessi et al. (1987) have proposed that the free solution realized in the inertial recirculation is the result of mixing the potential vorticity imported by the boundary current with the planetary vorticity present in this region. The potential vorticity imported by the separated boundary current is of southern (northern) origin in the subtropical (subpolar) gyre, and is therefore anomalously low (high). In the formulation of Cessi et al. (1987), only the subtropical gyre is considered and the anomalous potential vorticity produced by the nonlinear western boundary layer is simply prescribed at the northern edge of the recirculation gyre. The northern solid boundary mimics the latitude of separation of the western boundary current. In models such as that of Schmitz and Holland (1986), it coincides with the line of symmetry dividing the subpolar and subtropical gyre and with the latitude of zero wind stress curl. Thus, the body force due to the wind stress is neglected and the following "boundary-driven" model is used to describe the flow in the inertial recirculation region:

$$J(\psi, \nabla^2\psi + \beta y) = \kappa\nabla^2\zeta$$

$$\text{with} \quad \left.\begin{aligned}\psi &= 0\\ \zeta &= \zeta_b\end{aligned}\right\} \quad \text{on the boundary} \qquad (1.3)$$

where $\zeta_b(s)$ is a prescribed function of the arclength, s, along the boundary and the boundary itself has a simple geometry (a rectangle). In Cessi et al. (1987), ζ_b is a negative constant along the northern wall and vanishes along the southern wall so that the recirculation gyre extends all the way to the eastern wall, but occupies only a portion of the domain in the meridional direction, being bounded to the south by a free streamline. In the limit of vanishing diffusivity, κ, the flow within the recirculation gyre asymptotes to the inviscid free solution of (1.3) given by constant potential vorticity. The meridional extent of the boundary driven gyre and its potential vorticity is independent of κ, linearly proportional to the anomalous relative vorticity ζ_b injected at the northern boundary and inversely proportional to β. This free solution is realized only in the northern portion of the domain, while in the rest of the domain there is a very weak diffusive flow.

Ierley and Young (1988, hereafter referred to as IY) extended these calculations to include longitudinal dependence of the boundary forcing, by making ζ_b vanish in the eastern half of the northern wall as well as on the southern wall. In this case, the recirculating gyre does not fill the domain in the east–west direction and instead is bounded by a free streamline to the south *and* the east. The solution found by IY is interesting because both the streamfunction maximum and the gyre width decrease as the diffusivity, κ, is decreased, and yet diffusion remains subdominant in the interior of the gyre. In the interior of the gyre the "free" solution of the vorticity equation (1.3) with constant potential vorticity is obtained, but the constant value of the potential vorticity depends to first order on the diffusivity κ. The free solutions found in the region of homogenized potential vorticity owe their structure to the presence of the planetary vorticity gradient, β, which is erased by the relative vorticity gradient of the free flow. Both the case examined by IY and that considered by Cessi et al. are nongeneric because the forcing is applied along a latitude circle and thus along a line parallel to the lines of constant planetary vorticity, βy. We will show that when the geometry of the boundary-driven model examined by IY is varied by an infinitesimal amount the free inertial mode is no longer necessarily the asymptotic solution in the limit $\kappa \to 0$. Just as in the wind-driven model (1.1), a free solution can be realized only for certain geometries of the wind forcing, in the boundary-driven model (1.3) a free solution is found only for certain geometries of the boundary.

It is the goal of this work to examine which geometrical configurations allow the realization of a free solution in the inviscid limit. To do so, the geometry examined by IY is altered by rotating the boundary of the domain with respect to the lines of constant potential vorticity (see Fig. 1). This study shows that for any counterclockwise rotation ($\theta > 0$ in Fig. 1) the free inertial mode is no longer realized as the inviscid limit of the vorticity equation (1.3), and instead a nonlinear frictional solution is obtained.

2. Formulation of the model

Changes in the geometrical configuration of the boundary-driven model (1.3) are introduced through a single parameter, θ, which measures the rotation of the planetary vorticity contours with respect to the

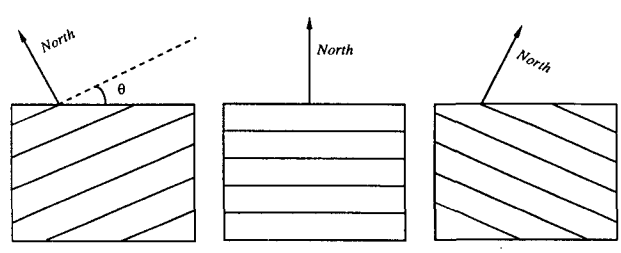

FIG. 1. Contours of planetary potential vorticity for different values of the angle θ: $\theta < 0°$ in the leftmost panel, $\theta = 0°$ in the center panel, and $\theta > 0°$ in the rightmost panel. In all cases the stress is applied at the upper left-hand corner of the boundary.

boundary where the forcing is specified. In this case the "boundary-driven" model is

$$J(\psi, q) = \kappa\nabla^2\zeta, \quad q \equiv \zeta + \beta y\cos\theta + \beta x\sin\theta \tag{2.1}$$

with $\left.\begin{aligned}\psi &= 0\\ \zeta &= \zeta_b\end{aligned}\right\}$ on the boundary.

The geometry of the domain and the lines of constant planetary vorticity are shown in Fig. 1. The y coordinate goes from $-L$ to 0 and the x coordinate from 0 to L/α, so that α is the aspect ratio of the box. The forcing ζ_b is identical to that used by IY:

$$\zeta_b = \begin{cases} \hat{\zeta}[\tanh(20\alpha x/L - 10) - 1]/2 & \text{at } y = 0\\ \hat{\zeta}\left[\dfrac{\tanh 2(y+L)/L}{\tanh 2} - 2(y+L)/L\right] & \text{at } x = 0\\ 0 \quad \text{otherwise.} \end{cases} \tag{2.2}$$

A graph of the boundary forcing ζ_b as a function of the arclength along the boundary is shown in Fig. 2. The forcing is essentially zero except in the upper left hand corner of the domain ($y = 0$, $x < L/2\alpha$).

For $\theta < 0°$ the forcing is effectively applied at the northeast corner of the domain, for $\theta = 0°$ at the northwest corner, and for $\theta > 0°$ at the southwest corner. For convenience we will from now on refer to the boundary $y = 0$ as the "northern wall."

In the wind driven model (1.1) the wind stress curl generates vorticity in the interior of the domain and, thus, the circulation occupies the whole box. In the boundary-driven model (2.1) and (2.2), in the limit $\kappa \to 0$, the vorticity prescribed at the wall may spread in the interior of the domain or may be confined to a thin diffusive boundary layer close to the forced boundary, depending on the sign of θ. The specification of negative relative vorticity (positive shear $\partial_y u$) on the northern boundary drives an eastward flow along the wall. The negative vorticity is advected eastward and diffused towards the interior of the domain where the mass is returned. Typical solutions for small diffusivity and two different geometries ($\theta < 0°$ and $\theta > 0°$) are shown in Fig. 3. For negative θ the flow extends considerably into the interior and its amplitude is large, while for positive θ the flow is confined to a thin, boundary layer near the northern wall and its amplitude is small. The solutions shown in Fig. 3 were found numerically using a spectral code, developed by G. R. Ierley, that solves (2.1) using Newton's method. A brief description of the method of solution can be found in Cessi et al. (1987).

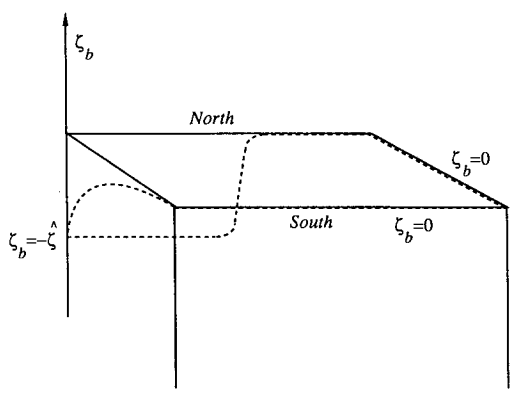

FIG. 2. A perspective plot of the boundary forcing ζ_b (dashed line). The forcing vanishes everywhere except at the northwest corner of the domain and is essentially constant on the westernmost half of the northern wall.

In the following we examine how the characteristics of the gyre such as its longitudinal and latitudinal extent, its transport and velocity depend on the parameters of the problem: the diffusivity κ, the amplitude of the forcing $\hat{\zeta}$, the geometry of the boundary expressed by the angle θ, and the length of the forcing region L/α. The symbols for the characteristic scale of the gyre's features are defined in the following and in Fig. 4, they will be used throughout the rest of the paper. We define

l the latitudinal width of the gyre

$\mathcal{L}$ the longitudinal width of the gyre

U the zonal velocity of the gyre. (2.3)

To determine whether the solution of the vorticity equation (2.1) asymptotes, in the inviscid limit, to a free solution we use the Reynolds number as a diagnostic:[1]

$$R \equiv \frac{t_{\text{diff}}}{t_{\text{adv}}}$$

where

$$t_{\text{diff}} \equiv l^2/\kappa$$

$$t_{\text{adv}} \equiv \mathcal{L}/U. \tag{2.4}$$

If the Reynolds number tends to infinity in the limit $\kappa \to 0$ then we decree that a free solution is obtained in the inviscid limit. For example, in the case examined by IY [obtained by setting $\theta = 0$ in (2.1)] the scale of the meridional width, l, is $(\kappa L/\alpha\hat{\zeta})^{1/6}(\hat{\zeta}/\beta)^{1/2}$, the scale of the zonal velocity U is βl^2, and the scale for the gyre length $\mathcal{L}$ is the length of the forcing L/α. Then the Reynolds number is $R = (\alpha\hat{\zeta}^4/\beta^3\kappa L)^{1/3}$ and becomes infinite in the inviscid limit. The prediction for the Reynolds number obtained by IY is confirmed by the numerical results shown in Fig. 5 (the experiments for $\theta = 0$ are indicated by the symbol $\times$). The Reynolds number in the numerical experiments is cal-

[1] Ierley and Young (1988) had a different definition.

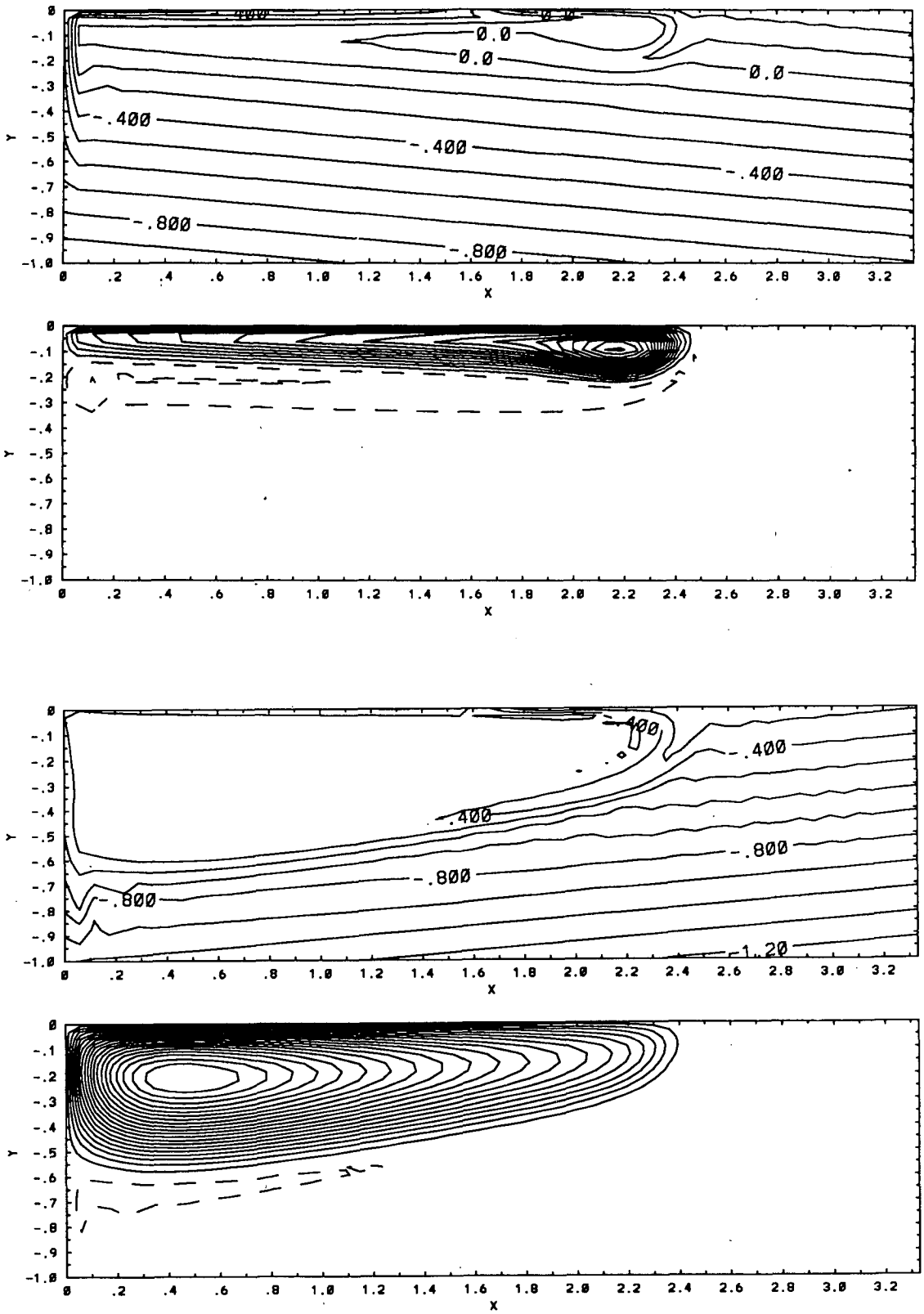

FIG. 3. Streamfunction and potential vorticity fields resulting from the numerical solution of (2.1) for different geometries: (a) potential vorticity for $\theta = 5°$, (b) streamfunction for $\theta = 5°$: dashed contours indicate negative values and the contour interval is 4×10^{-5}; (c) potential vorticity for $\theta = -5°$, (d) streamfunction for $\theta = -5°$: the contour interval is 3×10^{-4}. The potential vorticity field is presented in units of βL and the streamfunction is units of βL^3. For both geometrical configurations the amplitude of the boundary forcing is $\xi = \beta L/2$, the aspect ratio of the domain is $\alpha = 0.3$, and the diffusivity κ is $7.5 \times 10^{-6} \beta L^3$.

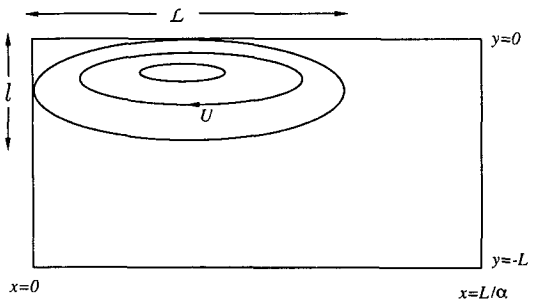

FIG. 4. A schematic view of the gyre forced by the boundary stress. The characteristic longitudinal extend of the gyre is $\mathcal{L}$, the characteristic latitudinal extent is l, and the typical zonal velocity of the gyre is U. The aspect ratio of the domain is α and in all the calculations presented here α is set equal to 0.3.

culated using the following prescription. We take the maximum zonal velocity (which always occurs on the northern wall) as the velocity scale U, we define the longitudinal scale $\mathcal{L}$ as the distance of the point of maximum zonal velocity, call it x_0, from the western wall ($x = 0$). Finally the scale of the gyre's width l is taken to be the distance from the northern wall of the point where the streamfunction changes sign at the longitude x_0.

3. Diffusive dynamics and the breakdown of the inviscid solution

As anticipated by the results shown in Figs. 3 and 5, when the planetary vorticity contours are rotated clockwise with respect to the forced boundary ($\theta > 0$ in the definition of the potential vorticity 2.1), the flow is weak and friction is dominant in the limit $\kappa \to 0$. A symptom of the dominance of viscosity is the fact that streamlines, shown in Fig. 3b, are crossing lines of constant potential vorticity, shown in Fig. 3a, throughout the gyre. It should be noted that for the same value of forcing amplitude, $\hat{\zeta}$, and diffusivity, κ, IY found that when $\theta = 0$ most of the flow occurs in a region of homogenized potential vorticity. A more quantitative measure of the importance of diffusion is the Reynolds number, which for positive θ, becomes independent of the diffusivity κ (the experiments with $\theta > 0$ are indicated by the symbols + and O in Fig. 5). In this case, no matter how small κ is, a free solution is never achieved.

The reason why even an infinitesimal but positive angle drastically changes the behavior of the solution as the diffusivity is decreased is simple. Along the northern wall the negative relative vorticity imposed at the boundary induces an eastward jet. Unlike the case examined by IY the planetary vorticity $\beta y \cos\theta + \beta x \sin\theta$ changes along the northern wall; for positive θ it increases towards the east. If the eastward flow were to conserve its potential vorticity, then the relative vorticity, ζ, would decrease to compensate for the increase in the planetary term. Thus, the shear $\partial_y u = -\zeta$ will increase as the fluid progresses eastward. This increment can be achieved in two ways. First, the width of the gyre can decrease, and this results in a reduced

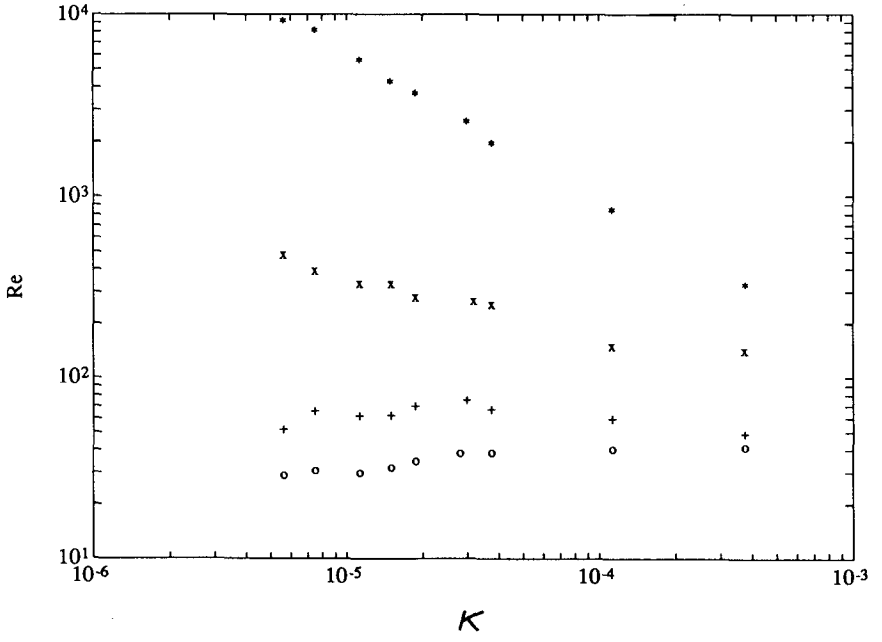

FIG. 5. Reynolds number as a function of the nondimensional diffusivity $\kappa/\beta L^3$ for different values of the angle θ. The symbol O denotes the results obtained for $\theta = 10°$, + is for $\theta = 5°$; for positive θ the Reynolds number is independent of the diffusivity κ. The symbol × denotes the results for $\theta = 0°$ previously analyzed by Ierley and Young (1988). The results obtained for $\theta = -5°$ are denoted by the symbol *; in this case the solution in the inviscid limit is independent of the diffusivity, so the Reynolds number is proportional to κ^{-1}.

scale separation between the "interior" of the gyre and the viscous sublayer close to the northern wall. Alternatively, the shear $\partial_y u$ can increase if the velocity increases while the width of the gyre remains approximately constant. If this is the case, then the velocity in the viscous sublayer must also increase. Because the vorticity in the viscous sublayer is determined by the boundary value, the width of the viscous sublayer must also increase to compensate for the velocity increase, once again resulting in an enhanced influence of friction. The same line of reasoning suggests that if the planetary vorticity *decreases* eastward (negative θ) then in the interior of the gyre the influence of friction should be diminished and indeed this is confirmed by the numerical results: the transport of the gyre shown in Fig. 3d is large and its potential vorticity (Fig. 3c) is constant. The results for $\theta < 0$ will be discussed in more detail in section 4.

An alternative point of view is provided by Welander's (1968) "thermal analogy." The (linear) pathways for propagation of information depend on the angle θ. With reference to Fig. 1, it is clear that when θ is negative, "westward" is directed away from the forcing into the interior. Thus, the stress of the boundary is communicated into the interior and establishes an inertial gyre. On the other hand, for positive θ, information propagates towards the boundary where the forcing is applied and, thus, the response is confined to a thin region near the wall where diffusion is important.

For positive θ, away from the region where the flow is turning, we can make use of the boundary layer approximation, and the flow is governed by

$$J(\psi, \partial_y{}^2, \psi) - \beta \sin\theta \partial_y \psi = \kappa \partial_y{}^4 \psi \qquad (3.1)$$

with boundary conditions $\psi = 0$ and $\partial_y{}^2\psi = \zeta_b$ at $y = 0$. Northward advection of planetary vorticity, $\beta \cos\partial_x\psi$, is subdominant because the flow is confined near a solid wall where the no-normal flow condition is applied. The length scale in the y direction is given by l and in the x direction by L/α, the length of the forcing, while the streamfunction ψ scales as $\hat{\zeta} l^2$. The size of each term in (3.1) is given by

$$\begin{aligned} &J(\psi, \partial_y{}^2, \psi) - \beta \sin\theta \partial_y \psi = \kappa \partial_y{}^4 \psi \\ &\hat{\zeta}^2 l\alpha/L \qquad\qquad \hat{\zeta}\beta \sin\theta l = \kappa\hat{\zeta}/l^2. \end{aligned} \qquad (3.2)$$

Diffusion is important everywhere and the ratio of the second to the first term on the left-hand side is $\beta L \sin\theta/(\alpha\hat{\zeta})$ and is small for small θ: the gyre consists of a nonlinear, viscous flow. If the forcing ζ_b is a constant, equal to $-\hat{\zeta}$, as the special form (2.2) is in the westernmost portion of the northern boundary, an exact nonlinear solution of (3.1) can be found for which the nonlinear term vanishes identically and diffusion is balanced by eastward advection of planetary vorticity. This solution is

$$\psi = -\frac{2}{\sqrt{3}} \hat{\zeta} l^2 e^{y/2l} \sin(\sqrt{3}y/2l) \qquad (3.3)$$

where

$$l \equiv \left(\frac{\kappa}{\beta \sin\theta}\right)^{1/3}$$

and is analogous to the Munk solution (Pedlosky 1978), except that here there is no net zonal flow between $y = 0$ and $y = -\infty$. Notice that in this special solution the width of the gyre is independent of the amplitude of the forcing, $\hat{\zeta}$, as in the linear case, and the Reynolds number is $R = \hat{\zeta}\alpha/(\beta L \sin\theta)$. The prediction that, for positive θ, the Reynolds number is inversely proportional to $\sin\theta$, is confirmed by the numerical results shown in Fig. 5: the Reynolds number

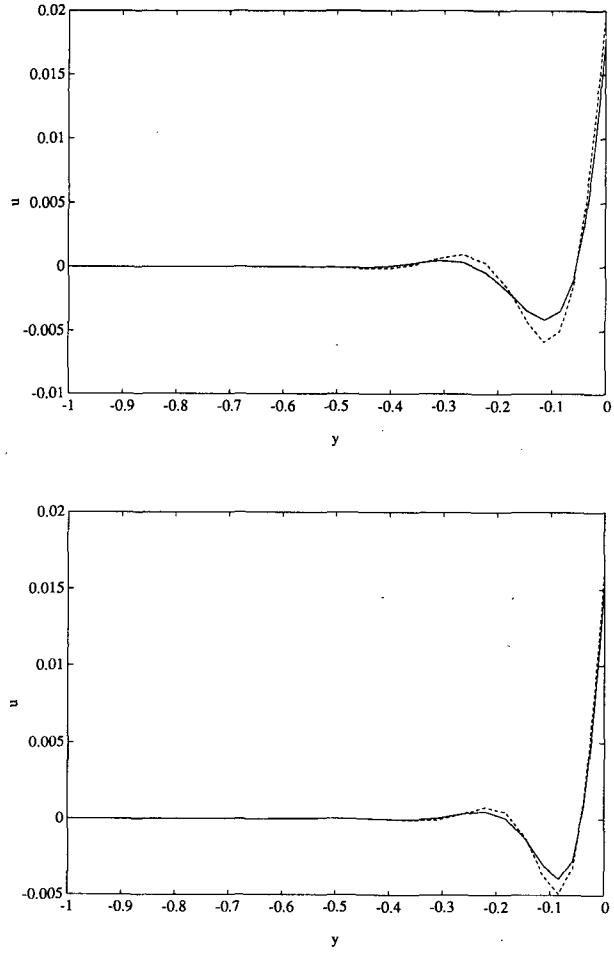

FIG. 6. Nondimensional zonal velocity $u/(\beta L^2)$ as a function of latitude y/L at the longitude of maximum velocity, x_0, resulting from the numerical solution (solid line) compared with the one-dimensional Munk solution (3.3) (dashed line). (Top) $\theta = 5°$. (Bottom) $\theta = 10°$. In both cases $\kappa = 7.5 \times 10^{-6}\beta L^3$. The amplitude of Munk solution has been corrected to allow for the fact that at $x = x_0$ the boundary value of relative vorticity, ζ_b, is slightly smaller than $-\hat{\zeta}$.

for the experiments with $\theta = 5°$ (denoted by +) is about twice the Reynolds number for the experiments with $\theta = 10°$ (denoted by O). Moreover, the one-dimensional solution (3.3) agrees quantitatively with the numerical solution at the longitude of maximum zonal velocity x_0 as shown in Fig. 6. For negative θ the solution (3.3) is not confined to the wall, the boundary layer approximation (3.1) fails and an inertial gyre is established.

4. The free, inertial solution

A typical solution, in the case where the planetary vorticity contours are rotated counterclockwise with respect to the boundary where the forcing is applied ($\theta < 0$), is shown in Fig. 3c,d. In contrast with the results for positive θ, the solution of (2.1) with $\theta < 0$ tends to a free solution in the inviscid limit, the boundary-forced gyre has constant potential vorticity and the Reynolds number increases as κ^{-1} (the experiments for $\theta < 0$ are denoted by an asterisk in Fig. 5). Unlike the case analyzed by IY, the homogenized value of potential vorticity does not, to first order, depend on κ and all the quantities characterizing the interior flow are, to leading order, independent of κ. Thus, the Reynolds number has a steeper dependence on the diffusivity than the configuration analyzed by IY.

This behavior was anticipated by the heuristic arguments presented at the beginning of section 3. For negative θ the stress is propagated from the region of forcing, which is effectively an eastern wall, into the interior and an inertial gyre is established. In the interior region the flow is governed by

$$\partial_x{}^2\psi + \partial_y{}^2\psi + \beta\cos\theta y + \beta\sin\theta x = \bar{q}. \quad (4.1)$$

A simple, exact solution of (4.1) can be found that satisfies the no-normal flow condition on the northern wall and has a free streamline at the unknown location $y = l(x)$. This solution is incomplete because it does not satisfy the boundary condition of no flow on the western wall. The expression for the streamfunction, away from the turning region near the western wall, is:

$$\psi = -\frac{\beta y}{12}(\cos\theta + \sqrt{\cos^2\theta - 3\sin^2\theta})(y - l)^2$$

where (4.2)

$$l = (\sqrt{\cos^2\theta - 3\sin^2\theta} - \cos\theta)(x - \bar{q}/\beta\sin\theta)/\sin\theta.$$

Here, $\bar{q}$ is the value of homogenized potential vorticity found in the interior which can be calculated using the "velocity weighted average" proposed by Cessi et al. (1987) and Mestel (1989):

$$\bar{q} = \frac{\oint q_b \mathbf{u}\cdot d\mathbf{l}}{\oint \mathbf{u}\cdot d\mathbf{l}} \quad (4.3)$$

where the contour integral is performed along the boundary of the domain. For an elongated gyre the main contribution to the integrals in (4.3) comes from the velocity along the northern wall, which can be calculated, except for a negligible region near the western wall, from (4.2). Then the constant value of potential vorticity is given by

$$\bar{q} \approx \frac{-\int_0^{L/2\alpha} \hat{\zeta}\,\partial_y\psi(x,0)dx + \int_0^{\bar{q}/\beta\sin\theta} \beta\sin\theta x\,\partial_y\psi(x,0)dx}{\int_0^{\bar{q}/\beta\sin\theta} \partial_y\psi(x,0)dx}. \quad (4.4)$$

To obtain (4.4) we have assumed that the relative vorticity specified on the boundary is a constant given by $-\hat{\zeta}$ for $0 \leq x \leq L/2\alpha$ and vanishes elsewhere. Exploiting the smallness of the angle θ, the expression for the homogenized potential vorticity, $\bar{q}$, can be approximated with

$$\bar{q} \approx -\sqrt{-2\hat{\zeta}\beta\sin\theta L/\alpha}. \quad (4.5)$$

Notice that in the limit of vanishing θ we recover the IY result that the constant value of potential vorticity vanishes to order κ^0 and that the expression (4.5) is not valid for positive θ. For arbitrary negative angle $\bar{q}$ is of the order of $\hat{\zeta}$ and the width of the gyre l is of the order of $\bar{q}/\beta$, independent, to leading order, of the diffusivity.

An example of the free mode solution, (4.2), with the constant potential vorticity, $\bar{q}$, given by (4.5) is shown in Fig. 7. For the parameters' values $\alpha = 0.3$, $\hat{\zeta} = \beta L/2$ and $\theta = -5°$, corresponding to parts (c) and (d) of Fig. 3, the homogenized value of potential vorticity found numerically is $\bar{q} = -0.48\beta L$ and this compares reasonably well with the approximate formula (4.5), which gives $\bar{q} \approx -0.54\beta L$. As mentioned earlier, the solution (4.2) is inadequate near the western wall because it doesn't satisfy the no-flow boundary condition there. Comparison with the numerical solution shown in Fig. 3d suggests that the inertial solution (4.2) is also substantially modified by diffusion in the region where the inertial flow is the weakest, i.e.,

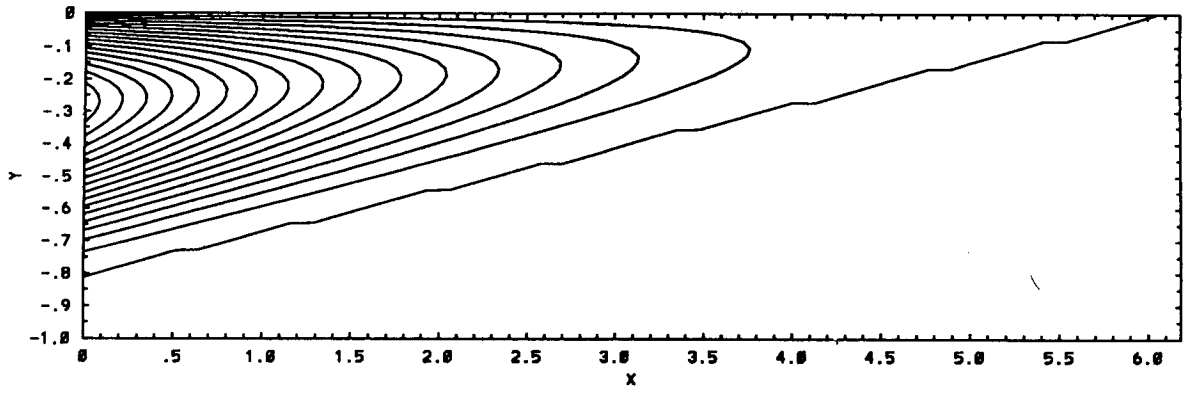

FIG. 7. The free mode solution (4.2) in units of βL^3 for the parameters' values $\alpha = 0.3$, $\theta = -5°$, $\hat{\xi} = \beta L/2$. The contour interval is 1×10^{-3}. Notice that the meridional scale has been expanded by a factor of two for clarity and the gyre extends up to $x = 6.2L$ in the x-direction.

in the eastern region of the wedge. Because the velocity in the tip of the wedge is very weak, its value does not affect the velocity weighted average (4.3), and it is not surprising that, despite the disagreement in the flow structure here, the prediction of $\bar{q}$ given by (4.5) agrees quite well with the numerical solution in Fig. 3c.

5. Conclusions and conjectures on the implications for the ocean

We have shown that the existence of a free solution in the inviscid limit of the quasi-geostrophic equation on a β-plane depends on the geometry of the forcing. We have examined a particular problem where the flow is forced by a stress applied on the boundary and the geometry of the problem is described by a single parameter: the angle θ between the planetary vorticity contours and the boundary where the stress is applied. In the case where θ is negative (see Fig. 1) the flow organizes itself in a gyre whose characteristics are, to leading order, independent of the diffusivity κ and so the Reynolds number becomes infinite in the inviscid limit. In the case where θ is positive the Reynolds number is independent of the diffusivity, the flow is confined to a diffusive boundary layer and does not approach a free solution as $\kappa \to 0$. The case $\theta = 0$, previously analyzed by Ierley and Young (1988), is very special because in the core of the flow diffusivity is negligible and the Reynolds number diverges in the inviscid limit, and yet the characteristics of the gyre depend to leading order on κ. Thus, the asymptotic behavior for vanishing κ is discontinuous at the point $\theta = 0$. We conclude that equations (1.3) and (2.1) are singular in the limit $\kappa \to 0$, and that, in general, the assumption that a free flow is obtained in the inviscid limit cannot be taken lightly.

The distinction between the free, inertial response shown in Fig. 3d and the diffusive gyre shown in Fig. 3b is important because in the former case the transport of the gyre is much larger than in the latter. The inertial or diffusive character of the flow is evident only for small enough values of the diffusivity κ, while for moderate viscosity there is little difference between the results at a small positive angle and those at a small negative angle. This is why, although we have varied κ by two decades, we have focussed our discussion on the most inviscid regime. As modelers, we are interested in the inviscid limit of the vorticity equations as a useful paradigm of the strongly nonlinear regime. One of the advantages of the boundary-driven model (2.1) over a wind-driven model is that it allows a thorough exploration of the parameter space. Because it is a "regional," steady model we can afford many experiments at a rather small value of diffusivity, although we haven't yet reached true asymptopia.[2] The smallest value of κ that we have used is $5.6 \times \beta L^3$ which, for $L = 1000$ km, gives 112 $m^2\ s^{-1}$, which is as small as the explicit lateral diffusivity used in very expensive wind driven eddy resolving general circulation models (ERGCM) (the value used by Lozier and Riser (1989) is 100 $m^2\ s^{-1}$). Of course in these wind driven ERGCMs the flow is baroclinic, time dependent, and the rich eddy field present in the recirculation region may change the value of the effective diffusivity and comparison with our steady, boundary driven model becomes more difficult.

Despite the model's obvious limitations, our results are relevant for the recirculation gyres seen in ERGCMs in which the line where the wind stress curl changes sign is not aligned with a latitude circle. In this case the linear, Sverdrup theory predicts that the separated boundary current flows along a line which is not parallel to a latitude circle. The literature on wind driven flow with such a "tilted" wind stress profile is sparse, but preliminary results of P. B. Rhines and R. Schopp seem to support that in the nonlinear regime the gyres' geometry is preserved (in a time averaged sense) and the

[2] Asymptopia: word coined by Glenn R. Ierley to denote the ideal condition in which even $\epsilon^{1/15}$ is much smaller than one.

anomalous values of potential vorticity produced in the nonlinear western boundary layer are carried along a line which is tilted with respect to βy. The path of the separated boundary current then plays the role of the "northern (southern) wall" for the subtropical (subpolar) gyre along which the relative vorticity is anomalously low (high). If the path of the separated boundary current veers northeastward, then the "forced boundary" is rotated counterclockwise with respect to a latitude circle in the subtropical gyre, and clockwise in the subpolar gyre. Our result would then suggest that in the recirculation gyre generated to the north potential vorticity is approximately conserved, while to the south the recirculating gyre is dominated by diffusion. It is possible then that the stability properties of the recirculating flow are quite different in the two regions because of the different dynamical balances.

Acknowledgments. We are very grateful to Glenn R. Ierley for generously making his numerical code available to us. Glenn Flierl kindly let us use his Sun Workstation for the preliminary calculations and William R. Young cheerfully agreed to have his Sun Workstation clogged with the calculations presented in this work. This work was undertaken while the authors were participants in the 1989 Geophysical Fluid Dynamics Summer Program, Woods Hole, Massachusetts, which is supported by the National science Foundation. A preliminary report of this work appears in the Fellows Projects Report of that year. We also wish to acknowledge NSF OCE-8901720 (PC) and ONR-N00014-86-K-0325 (LT).

REFERENCES

Cessi, P., G. Ierley and W. Young, 1987: A model of the inertial recirculation driven by potential vorticity anomalies. *J. Phys. Oceanogr.*, **17,** 1640–1652.

Fofonoff, N. P., 1954: Steady flow in a frictionless homogeneous ocean. *J. Mar. Res.*, **13,** 254–262.

Greatbatch, R. J., 1987: A model for the inertial recirculation of a gyre. *J. Mar. Res.*, **45,** 601–634.

Griffa, A., and R. Salmon, 1989: Wind-driven ocean circulation and equilibrium statistical mechanics. *J. Mar. Res.*, **47,** 457–492.

Ierley, G. R., and W. R. Young, 1988: Inertial recirculation in a β-plane corner. *J. Phys. Oceanogr.*, **18,** 683–689.

Lozier, M. S., and S. C. Riser, 1989: Potential vorticity dynamics of boundary currents in a quasi-geostrophic ocean. *J. Phys. Oceanogr.*, **19,** 1373–1396.

Marshall, J., and G. Nurser, 1986: Steady, free circulation in a stratified, quasi-geostrophic ocean. *J. Phys. Oceanogr.*, **16,** 1799–1813.

——, 1988: On the recirculation of the subtropical gyre. *Quart. J. Roy. Meteor. Soc.*, **114,** 1517–1534.

Mestel, A. J., 1989: An iterative method for high-Reynolds-number flows with closed streamlines. *J. Fluid Mech.*, **200,** 1–18.

Niiler, P. P., 1966: On the theory of wind driven ocean circulation. *Deep-Sea Res.*, **13,** 597–606.

Pedlosky, J., 1978: *Geophysical Fluid Dynamics.* Springer-Verlag, 624 pp.

Schmitz, W. J., Jr., and W. R. Holland, 1986: Observed and modeled mesoscale variability near the Gulf Stream and Kuroshio extension. *J. Geophys. Res.*, **91,** 9624–9638.

Welander, P., 1968: Wind-driven circulation in one- and two-layer oceans of variable depth. *Tellus,* **20,** 1–15.